Compton

Physics Laboratory report

Group 28: Attilio Crognale and Javier Mariño Villadamigo

December 17, 2021

Contents

1 Introduction

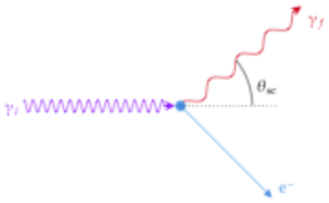

Figure 1: Kinematics diagram for Compton scattering.

Compton scattering is one of the most simple yet important processes in particle physics. The kinematics of the interaction is depicted in Fig. 1, where a photon γ_i with energy E_i scatters an electron (essentially at rest) to transfer E_e energy to it. The final photon is scattered with an angle of θ_{sc}, having a final energy of E_f. Applying energy and momentum conservation, the formula that connects both photon energies and the scattering angle is:

$$\frac{1}{E_f} - \frac{1}{E_i} = \frac{1}{m_e c^2}(1 - \cos\theta). \tag{1}$$

The main goals of this experiment are, then, to verify that energy distributions of the scattered photon and electron follow the theoretical behavior given by Eq. 1, and to measure the cross-section of the process at a given angle and compare the result with the value obtained using the Klein-Nishina cross-section formula:

$$\left(\frac{d\sigma}{d\Omega}(\theta)\right)_{\mathrm{KN}} = \frac{e^4}{2m_e^2c^4}\left(\frac{E_f}{E_i}\right)^2\left(\frac{E_f}{E_i} + \frac{E_i}{E_f} - \sin^2\theta\right). \tag{2}$$

2 Experimental setup

In this experiment, the photon source is a sample of ^{22}Na, which decays β^+ emitting a positron that, once annihilated with an electron, emits two back-to-back 511 keV photons (which will be crucial for the taggering of the events). The final state of this decay is primarily an excited state of ^{22}Ne, and the latter de-excitates emitting one photon of about 1.2 MeV. The remaining components of the experimental setup are:

- Three inorganic scintillator detectors of NaI(Tl), from now on labelled TAGGER, SCATTERER and DETECTOR, coupled to their respective photomultipliers.
- A FAN-IN-FAN-OUT (FIFO) module.
- Three constant fraction time discriminators (one for each detector) that are used to get an output independent from the amplitude of the input signal.

- A coincidence unit, to implement logic gates.
- A digitizer, to acquire the signal in a human-readable way.
- A CAEN scaler module used to count directly the number of events.
- A ^{241}Am source used for the calibration of the detectors at low energies.

3 Calibration of the detectors

To setup the electronics before the proper measurements needed for calibration, it is first needed to make sure the CFTD has an adequate value of the threshold. To do this, a first FAN-IN-FAN-OUT output of the TAGGER is sent to the oscilloscope in order to visualize the signal. Another output is then sent to the CFTD and the prompt output of the latter is connected to the second oscilloscope channel. The CFTD threshold is then adjusted to provide an output only if the first signal has a certain minimum amplitude. This threshold is set as low as possible (it will be needed to measure low energy values in the case of the SCATTERER at 0 degrees configuration) while not triggering on electronic noise.

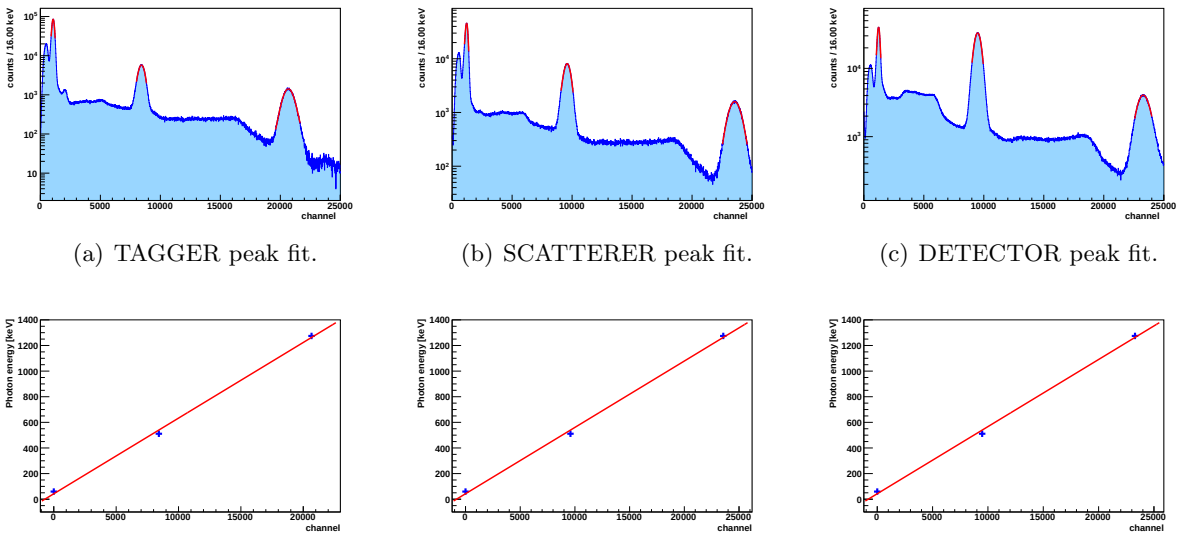

(a) TAGGER peak fit. (b) SCATTERER peak fit. (c) DETECTOR peak fit.

(d) TAGGER calibration. (e) SCATTERER calibration. (f) DETECTOR calibration.

Figure 2: Peak fit (upper row) and fit to the nominal values of peaks (lower row) of the 3 main peaks observed for each detector.

Once the CFTD threshold is correctly set, the anode signal from the FIFO of the TAGGER is connected to input 1 of the digitizer, and the delayed output (with minimum delay) is directed to the logic unit with fold 1 selection. The output of the logic unit will be then the trigger for the digitizer acquisition. Once everything is set up, a spectrum is recorded with an ^{241}Am and

a ^{22}Na sources. Repeating this process for SCATTERER and the DETECTOR, the calibration is ready to be taken care of.

# Detector	59 keV	511 keV	1275 keV	$E = a + b \cdot ch$	
	Res. (%)	Res. (%)	Res. (%)	a	b
TAGGER	23.9(2)	8.0(2)	4.97(4)	42(30)	0.059(2)
SCATTERER	21.5(3)	7.5(1)	5.18(6)	43(30)	0.052(2)
DETECTOR	21.4(3)	7.95(8)	5.7(2)	43(30)	0.052(2)

Table 1: Results of the calibration of the detectors. The three peaks of the sources were properly fitted to a gaussian curve with good χ^2/NDf values, obtaining better resolutions for the most energetic one. The equivalence of channel *vs* energy is shown in the last two columns, which will be used for the rest of the experiment.

In this sources configuration, 4 photons are expected. However, the least energetic one from ^{241}Am caused several fitting issues and was therefore discarded. This way, the only peaks taken into account were the 59.54092(10) keV one from the decay of ^{241}Am to ^{237}Np and posterior de-excitation[1], 511 keV from the annihilation of positronium proceeding from ^{22}Na, and 1274.537(7) keV from ^{22}Ne de-excitation. Each peak was fitted using a gaussian distribution plus a first degree polynomial in order to obtain the centroid, associated to a specific energy. The acquired data was compared with the known information about the values of the energies, and it was therefore possible to obtain the conversion function from channel to energy.

4 Statistics of the detectors

Because of the limited time available for the data acquisition, it was fundamental to set adequate run times. A good criteria for setting the duration of the acquisitions was found by studying the statistics in the detectors. In this part, only the DETECTOR was used. A set of acquisition runs was performed, and for each acquisition the spectrum of the DETECTOR was recorded. Each spectrum presented the 511 keV peak and a different amount of total events. for each spectrum the peak at 511 keV was fitted with a gaussian distribution obtaining the value of the centroid and its standard deviation, $C \pm \sigma$. The percentage error was then derived as $\sigma_C(\%) = \frac{\sigma}{C}$ and plotted with respect to the total number of events recorded in the spectrum N_{tot}, Fig. 3.

The percentage error follows the expected behavior given by a Poisson distribution. Taking advantage of the information shown in Fig. 3, the run time for each acquisition was set. In general the goal was to have at least 2000 events in each spectrum, resulting in a percentage error of about 0.9%.

[1]This peak is taken into account to improve the calibration at lower energies.

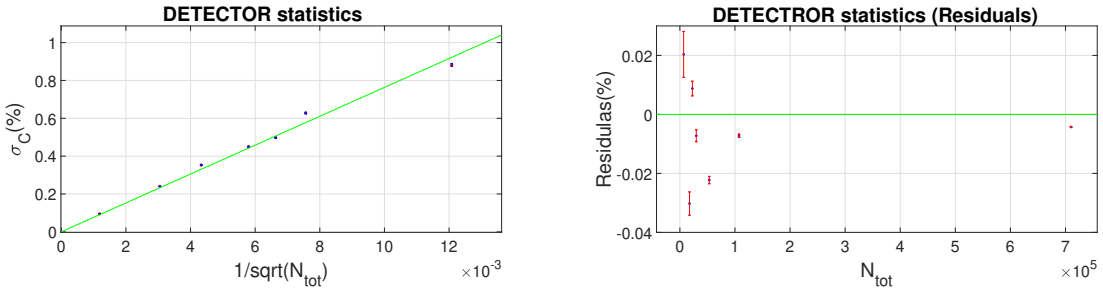

Figure 3: Error of the 511 keV peak with respect to the total events

5 Energy distribution

The first part of the experiment aims to study the energy of the scattered photon as a function of the scattering angle. To achieve this, the apparatus was arranged as follows: the TAGGER and the SCATTERER were placed at opposite sides of the ^{22}Na source. The DETECTOR was placed on a steel guide that allowed it to be moved around the SCATTERER, varying the angle with respect to it while keeping the same distance. It was therefore possible to change both the distance between DETECTOR and SCATTERER and the angular position of the DETECTOR. The ^{22}Na source was surrounded by lead bricks, and collimated in a circular beam of diameter $\Phi < 3.5$ cm. The spectra of all three detectors were acquired at a set of angles of $\theta = \{0,\ 20,\ 40,\ 60,\ 90,\ 100\}$ deg. The MASTER TRIGGER for the acquisition was set to be the coincidence between TAGGER, SCATTERER and DETECTOR. Ideally, the ^{22}Na would produce two back-to-back 511 keV photons. One of the photons would be detected by the TAGGER, while the second one would travel towards the SCATTERER and interact via Compton scattering, resulting in a moving electron and a deviated photon. The electron would then be reabsorbed in the SCATTERER while the photon would be detected by the DETECTOR placed at a certain angle. In general, the sum of the energies measured in the SCATTERER and the DETECTOR should be equal to 511 keV.

5.1 Geometrical discussion

However, the experimental setup has a certain angular acceptance, and it is therefore needed an in-deep analysis of the geometry features to accept the events that are properly energy-distributed. To do that, it is useful to take a look at the diagram depicted in Fig. 4. It is interesting to note that in this diagram, a non point-like source is used. The analysis that follows is particularized to the case in which the scattered photon is received at the end of the process in the DETECTOR, with a scattered angle that differs as much as possible from the angular position of the detector (i.e. this analysis tries to obtain the maximum angular acceptance of the detector for a certain angular position). First, the distances between TAGGER-Source (D_1), between Source-SCATTERER (D_2) and between SCATTERER-DETECTOR (D_3) were measured. Assuming a triangular distribution ($u(D) = \Delta D/\sqrt{24}$), the following distances for

this part of the experiment are obtained using $\Delta D = 5$ mm:

$$D_1 = 37(1) \text{ mm}, \qquad D_2 = 54(1) \text{ mm}, \qquad D_3 = 260(1) \text{ mm}.$$

With this configuration and knowing that the detectors have a diameter of 8 cm, a photon that is emitted at the maximum possible angle (and in the edge of a collimated beam of $\Phi < 3.5$ cm) while also intercepting the SCATTERER forms an angle of $\theta_1 = \arctan 4/3.757 \approx 46.8\,\text{deg}$. Then, the angular aperture subtended by the DETECTOR from the point of the scatter with respect to the horizontal line is $\Delta\theta = \arctan 8/26 \approx 17.1\,\text{deg}$. Finally, the angle of the "extreme" scattered photon as a function of the the detector angle is expressed as follows:

$$\theta_{\text{sc}}^{\text{max, min}} = \theta_D \pm (\theta_1 + \Delta\theta) \approx (\theta_D \pm 63.9)\,\text{deg}\,. \tag{3}$$

5.2 Selection of events

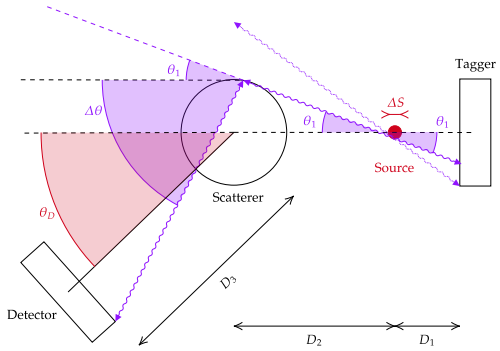

Figure 4: Geometrical configuration of the experiment, where the final photon is received in the detector placed at an angle θ_D, and was scattered with an angle $\theta_{\text{sc}} = \theta_1 + \Delta\theta$.

To illustrate how to proceed with the configuration of energy windows in the radiation spectra, the Fig. 5 is shown. First, an interval within $(3\cdot\sigma)$ from the 511 keV peak is selected in the TAGGER spectrum (Fig. 5(b) left) for the value of E_i. Then, according to Eq. 1, a corresponding range is obtained for E_e:

$$E_{\text{e}} = E_i \left[1 - \frac{1}{1 + \frac{E_i}{m_{\text{e}}c^2}(1 - \cos\theta)}\right] = \\ = E_i \left(1 - \frac{1}{2 - \cos\theta}\right), \tag{4}$$

where it was used that, in this experiment, E_i is expected to be exactly equal to $m_{\text{e}}c^2$. Of course, given the fact that $\cos\theta$ has a maximum for $\theta = 0$, then if $\theta_{\text{sc}}^{\text{min}}$ calculated according Eq. 3 is negative, $\theta_{\text{sc}}^{\text{min}} = 0$ is set.

Finally, the events in the DETECTOR that are in time coincidence with the events selected in Fig. 5(b) (left) and Fig. 5(b) (center), are taken into account to fill the histogram in Fig. 5(b) (right).

5.3 Correlation between the scatterer and detector

Logically, the sum of the energy of the electron and the energy of the final photon should sum up, for each event, to 511 keV, given the fact that the electron is initially considered at rest, and only the events that had 511 keV in the TAGGER were selected. To check if this is indeed correct, a correlation plot is done, where the DETECTOR energy is represented against the SCATTERER energy. This representation is shown in Fig. 6.

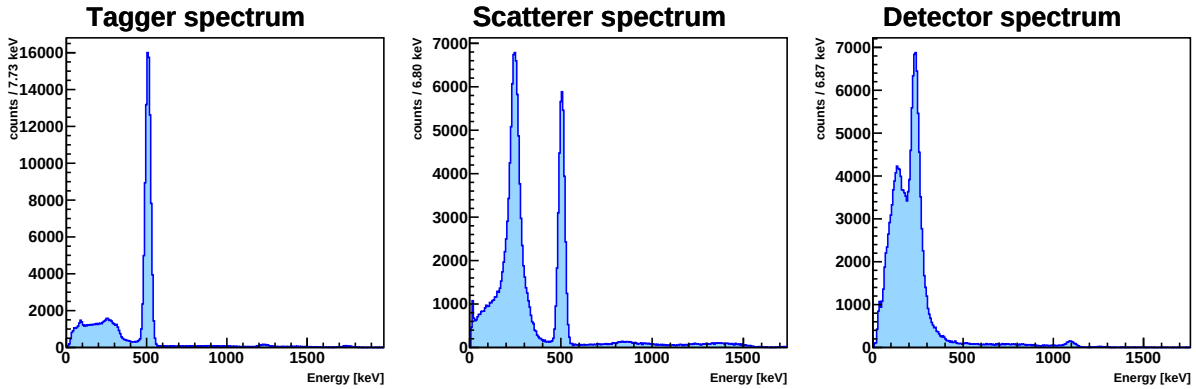

(a) Unfiltered events.

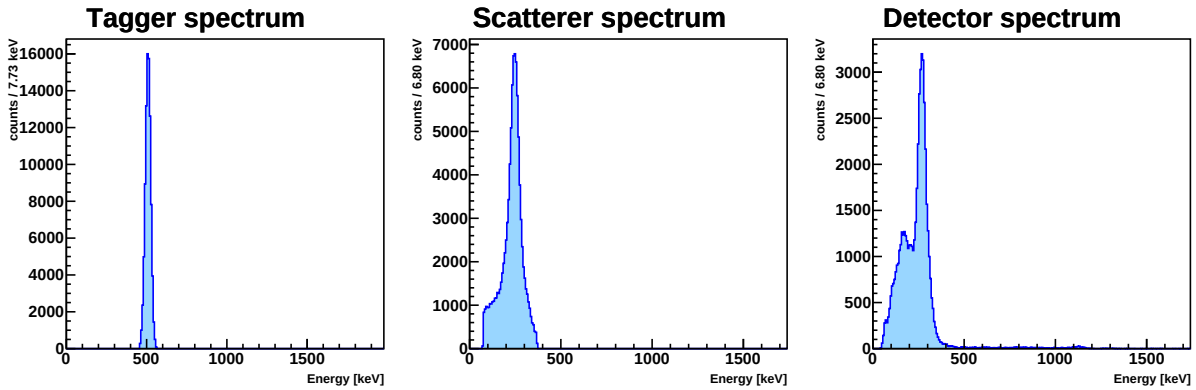

(b) Filtered events.

Figure 5: Unfiltered (upper) and filtered (lower) events for all three detectors at $\theta_D = 100\,\text{deg}$.

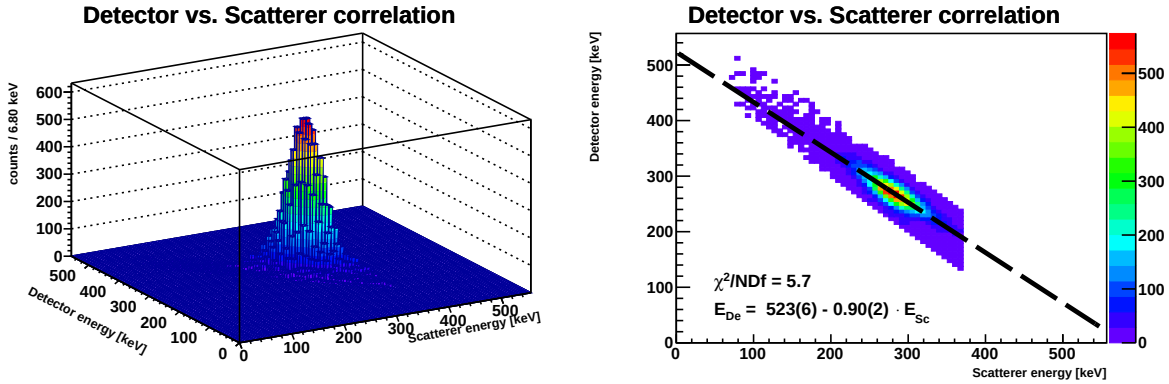

Figure 6: Correlation plots between energy of the scattered photon (DETECTOR) and the energy of the electron (SCATTERER). On the left, a three-dimensional plot is shown, where the number of counts is coded in a blue-to-red scale, while on the right the same information is represented in a two-dimensional plot, using the same color scale.

As it can be seen from Fig. 6, the energies of the events in the detectors are clearly correlated in a linear dependence with one another. An ideal fit would give an offset of 511 keV and a slope of -1. However, our results of the fit are:

$$E_{\mathrm{De}} = 523(6) - 0.90(2) \cdot E_{\mathrm{Sc}}, \qquad \chi^2/\mathrm{NDf} \approx 6;$$

which are not ideal, but are indeed in good agreement with what is expected. A slope that is not -1 could indicate a possible problem in the angular displacement of the DETECTOR around the SCATTERER which, as it was checked, was not perfectly centered on the axis of rotation of the DETECTOR, therefore the real θ_D was not exactly the measured one. The discrepancies with the offset value seem to be more subtle, and therefore their causes can range from an imprecise calibration to a systematic error in the angular analysis. The plots for the remaining angles are shown in the Appendix.

5.4 Energies of the scattered photon and of the electron as a function of the scattering angle θ

As commented in the previous section, an ideal correlation between the events registered in the DETECTOR and in the SCATTERER would always sum up to 511 keV in the case of an initial photon proceeding from the annihilation of an electron and a positron. To perform this analysis, the main peaks in the SCATTERER and DETECTOR filtered histograms (see Fig. 5(b) center and right, respectively) were fitted to gaussian distributions. The mean and the standard deviation provided by these fits are shown as the data points and their respective uncertainties in Fig. 7.

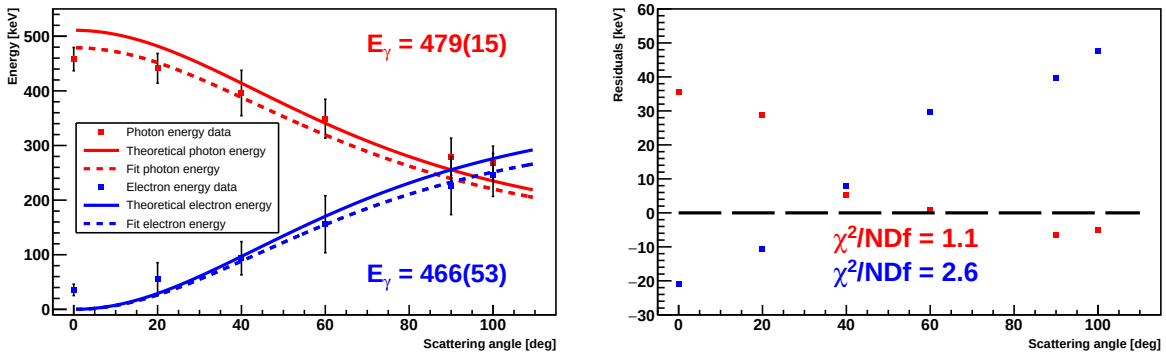

Figure 7: Dependence on the scattering angle θ of the energy of the scattered photon (red) and of the energy of the electron (blue). The solid lines on the left plot indicate the theoretically expected value, while the dashed lines are fits leaving E_i as a free parameter, whose result is shown in red and blue, respectively. On the right, the plot of residuals for both fits.

For comparison, the solid lines show the theoretical values expected calculated from Eq. 4 (blue) and the energy of the scattered photon that is computed as:

$$E_f = \frac{E_i}{2 - \cos\theta}. \tag{5}$$

In both cases a fit to the experimental values was also carried out, leaving E_i as a free parameter. The resulting fits provide very good values of χ^2/NDf, but the numerical values of the initial photon energy are deviated downward from the theoretical expectation of 511 keV. This means that the energy spectrum of the detector, mainly at lower angles, is shifted towards the left (or lower energies). This could be due to the fact that the cross-section at lower angles varies more rapidly than at higher angles, and could therefore lead to a less precise correction for the angular aperture. In any case, the correlation between the SCATTERER and the DETECTOR following Eqs. 5 and 4 can be considered proven in Fig. 7, as well as a linear relation between each other in good agreement with the theory, showed in Fig. 6.

6 Cross-section

The goal of the second part of the experiment is to measure the cross-section of the process at a fixed angle and then compare the result with the theoretical value given by the Klein-Nishina formula.

The set up for this second part is identical to the one used in the previous section except for two modifications: the SCATTERER was replaced by a sample of aluminum, and the MASTER TRIGGER was now set to be the coincidence between TAGGER and DETECTOR.

The experimental cross-section can be evaluated using the following formula:

$$\left[\frac{d\sigma(\theta)}{d\Omega}\right]_{\text{exp}} = \frac{\Sigma_\gamma}{\epsilon \cdot N_{\text{sample}} \cdot \Delta\Omega \cdot (I/S)}, \tag{6}$$

with:

- Σ_γ being the number of photons measured in the full-energy DETECTOR's peak.
- ϵ, the detection efficiency for photons of the DETECTOR.
- N_{sample}, the number of electrons in the aluminum sample.
- $\Delta\Omega$, the solid angle covered by the DETECTOR.
- $\frac{I}{S}$, the number of accidental photons per unit surface.

6.1 Detection efficiency for photons

In order to evaluate the detection efficiency ϵ, the aluminum sample was removed. The DETECTOR was then placed at an angular position of 0 deg and located as close as possible to the source. In this setup, all photons detected by the TAGGER should also be detected by the DETECTOR given the colinearity of the 511 keV photons. A spectrum was acquired both for the TAGGER and DETECTOR and two quantities were derived: N_{tot}, corresponding to the total number of

events detected in the TAGGER, and $N_1(511)$, corresponding to the number of events under the energy peak in the DETECTOR. The efficiency can be obtained as

$$\epsilon = \frac{N_1(511)}{N_{\text{tot}}} = 64.74(9)\%. \tag{7}$$

6.2 Photons in the DETECTOR's full-energy peak

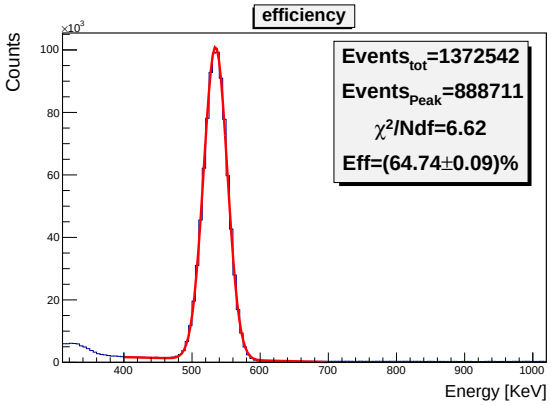

Figure 8: DETECTOR spectrum for the evaluation of ϵ.

The DETECTOR was placed at a distance of 260 mm from the scattering center, as previously done, and at an angular position of 100 deg. It is important to acknowledge one crucial fact: in this configuration the number of photons that are expected to be measured by the DETECTOR is relatively low. It is therefore fundamental to perform a background run, and to study the background spectrum. The acquisition yielded the result shown in Fig. 9(a). The background raises until about 180 keV, after this point the behavior seems to be exponential.

Once the background was acquired, the aluminum sample was reinserted. The final acquisition was carried out with the DETECTOR in the same position as before and the spectrum obtained for the DETECTOR is shown in Fig. 9(b).

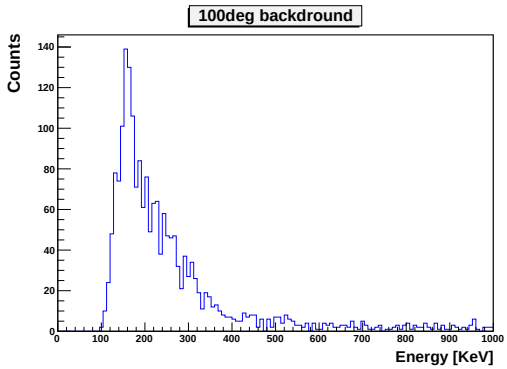

(a) Background spectrum at 100 deg.

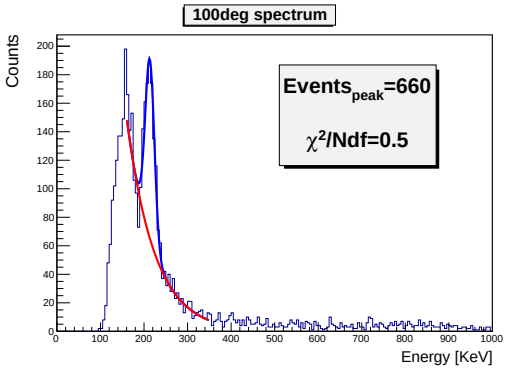

(b) Complete spectrum at 100 deg.

Figure 9: Acquired spectra for the measurement of the number of events in the main peak of the DETECTOR. On the left, the acquired background, while the spectrum on the right shows the gaussian plus background fit represented by the blue line, while the background alone is represented by the red line.

The photon peak is now visible and the region of the spectrum around 200 keV was fitted with a gaussian + exponential distribution, as suggested from the background. The value of Σ_γ can be obtained as the value of the integral of the gaussian distribution normalized to the value of a single bin. As shown in the spectrum, the result is $\Sigma_\gamma = 660(20)$.

6.3 Accidental photons

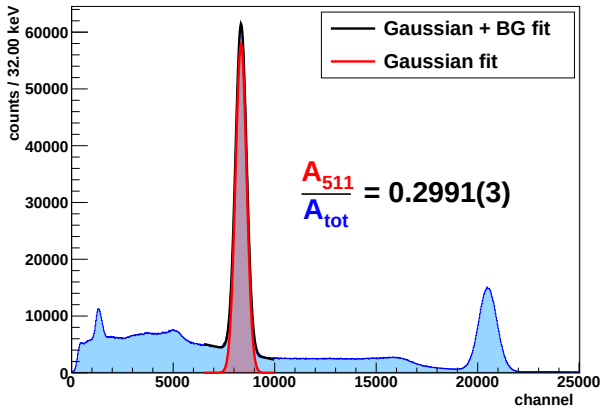

Figure 10: Spectrum acquired for the evaluation of the fraction $F(511)$. Note that the shaded area under the red curve represents the integral of the contribution to the full-energy peak, with a subtracted background.

The number of accidental photons was measured in the following way. The CFTD PROMPT output from the TAGGER was connected to the scaler counter. This made it possible to measure the number of photons in the TAGGER directly, bypassing the coincidence with the DETECTOR. The scaler counting for the events was carried out in parallel with the acquisition run that provided the results shown in Fig. 9(b). The number of accidental photons can be calculated as

$$I = N_{\text{scaler}} \cdot F(511), \tag{8}$$

where N_{scaler} is the output of the scaler unit (which amounted to $N_{\text{scaler}} = 24619(5) \cdot 10^3$), while the quantity $F(511)$ is defined as the ratio between the number of events under the 511 keV photopeak and the total number of events in the spectrum. In order to calculate $F(511)$, a separate spectrum was acquired for the TAGGER without implementing any logic gate. The photopeak was fitted to a gaussian distribution plus a first order polynomial. The integral of the gaussian (substracting the background represented by the first order polynomial) is defined as A_{511}, while the number of events in the spectrum is defined as A_{tot}. The results are summarized in Fig. 10.

The estimation of the accidental photons is therefore given by:

$$I = N_{\text{scaler}} \cdot F(511) = 7363(7) \cdot 10^3. \tag{9}$$

6.4 Numerical estimate of Compton cross-section

The remaining quantities needed for the evaluation of the cross-section were obtained trough simple hands-on measurement and geometrical considerations:

$$\Delta\Omega = 0.07(1)\ \text{sr}, \qquad N_{\text{sample}} = 7(1) \cdot 10^{24}, \qquad S = 50(2)\ \text{cm}^2.$$

The final experimental estimate for the cross-section is

$$\left.\frac{d\sigma}{d\Omega}\right|_{\text{exp},\ \theta=100\,\text{deg}} = 0.012(3)\,b = 1.2(3)\cdot 10^{-26}\ \text{cm}^2, \tag{10}$$

whereas the theoretical value from Klein-Nishina formula yields:

$$\left.\frac{d\sigma}{d\Omega}\right|_{\text{th},\ \theta=100\,\text{deg}} \approx 0.013639\,b = 1.3639\cdot 10^{-26}\ \text{cm}^2. \tag{11}$$

The experimental value is compatible with the theoretical one, verifying the validity of the Klein-Nishina formula. However the measurement itself is not particularly satisfying, considering that the error is about 25% of the obtained value.

7 Conclusions

To finalize and as a conclusion, it can be stated that the results obtained in the analysis of the angular dependence of the energy distribution are in reasonably good agreement with the theory, with the exception of a shift of the final photon to lower energies (and the electron to higher energies) at lower angles. This can be explained from a calibration flaw, but also from the difficulty of measuring very low energies at the scatterer. However, the results are considered to be satisfactory.

As to the cross-section, thanks to the background run, it was possible to filter properly the number of events in the full energy peak at 100 deg. The cross-section estimated experimentally matches the theoretical value within one σ, reinforcing the validity of Klein-Nishina formula. However, as stated before, the measure is not particularly precise because of the magnitude of the error.

8 Appendix: correlation plots

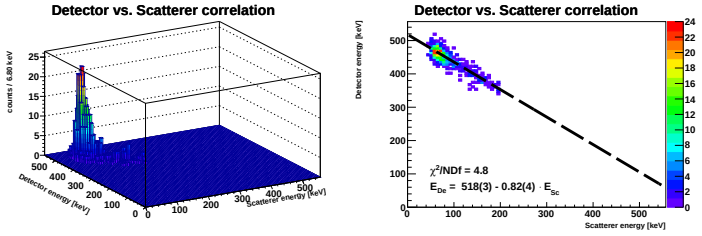

Figure 11: Correlation plots between energy of the scattered photon (DETECTOR) and the energy of the electron (SCATTERER) for 0 deg.

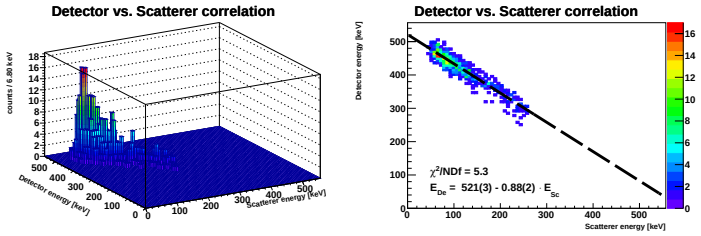

Figure 12: Correlation plots between energy of the scattered photon (DETECTOR) and the energy of the electron (SCATTERER) for 20 deg.

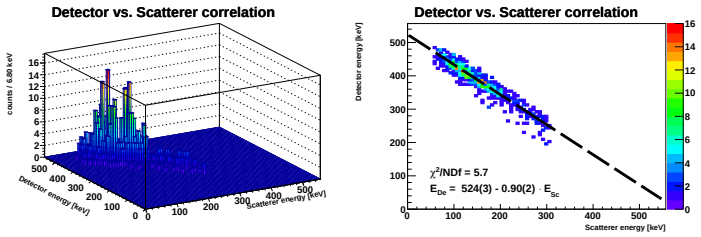

Figure 13: Correlation plots between energy of the scattered photon (DETECTOR) and the energy of the electron (SCATTERER) for 40 deg.

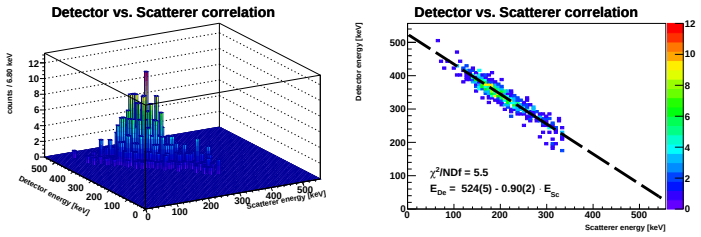

Figure 14: Correlation plots between energy of the scattered photon (DETECTOR) and the energy of the electron (SCATTERER) for 60 deg.

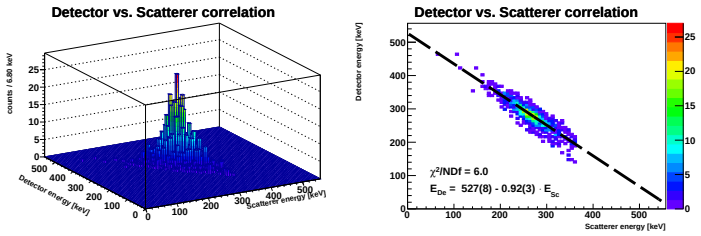

Figure 15: Correlation plots between energy of the scattered photon (DETECTOR) and the energy of the electron (SCATTERER) for 90 deg.